EXHIBIT A

A Method to Reduce the Probability of Clipping in DMT-Based Transceivers

Denis J. G. Mestdagh and Paul M. P. Spruyt

***Abstract*—A new method allowing a reduction in the probability of clipping in discrete multitone (DMT)-based transceivers is described. The method does not use any kind of precoding and can easily be implemented within conventional DMT-transceivers. The main advantage of the proposed method is an improvement of system performance in terms of overall signal-to-noise ratios (SNR's): with the simplest implementation option of the proposed method, up to about 8 dB improvement in the SNR as compared with previously reported brute force clipping methods can be achieved.**

I. Introduction

THE *discrete multitone* (DMT) modulation technique is emerging as a very powerful technique for applications ranging from asymmetric digital subscriber line (ADSL), digital audio broadcast (DAB) to interactive video on demand (IVOD) over CATV networks [1]–[3].

A DMT signal is the sum of N independently quadrature amplitude modulated (QAM) signals each being carried over a distinct carrier frequency. The frequency separation of the N carriers is equal to $1/T$ where T is the time duration of a DMT symbol. The real part of the complex envelope of the generated DMT signal can be expressed as

$$A(t) = \mathrm{Re}\left\{ \sum_{m=-\infty}^{+\infty} \sum_{k=0}^{N-1} [r_m^k \cdot e^{j2\pi(k/T)t} \cdot u(t - mT)] \right\} \quad (1)$$

where r_m^k denotes the QAM-phasor of carrier k (at frequency k/T) of the m-th DMT symbol and $(u)t$ is a rectangular transmit pulse of duration T.

In a practical transceiver, the DMT symbol (1) is generated by means of an inverse fast Fourier transform (IFFT) on the complex phasors $\{r_m^k\}, k \in [0, N-1]$ [4].

Fig. 1 shows the instantaneous amplitude $A(t)$ of two DMT symbols generated with two distinct sets of QAM-phasors $\{r_m^k\}_1$ and $\{r_m^k\}_2$, and $N = 256$. For both symbols, 16-QAM carrier modulation is assumed. A noticeable feature of the symbol in Fig. 1(b) as compared with the one in Fig. 1(a) is that it exhibits large amplitude spikes which arise when several frequency components add in-phase. These spikes may have a serious impact on the design complexity and feasibility of the transceiver's analog front-end (i.e., high resolution of D/A-A/D convertors and line drivers with a linear behavior over a large dynamical range). In addition, regulations can limit the peak envelope power or the probability of clipping [5]. The effect of amplitude clipping in DMT transceivers has been analyzed in the literature [6], [7] and methods based on encoding the input data in order to reduce the peak-to-average power ratio of the DMT signal have been proposed [8], [9]. The coding methods, however, require an increase in data rate and hence a reduction of the energy per bit for the same transmit power, resulting in performance degradation in terms of information handling capacity of the communication system.

In this letter, an alternative method is proposed. Since N is usually large (say $N \geq 128$), $A(t)$ can be accurately modeled as a Gaussian random process (central-limit theorem) with a zero mean and a variance σ^2 equal to the total signal power. Its probability density function (pdf), denoted as $p(x)$, is given by [6]

$$p(x) \cong \frac{1}{\sigma\sqrt{2\pi}} \cdot e^{-(x^2/2\sigma^2)}. \quad (2)$$

Therefore, large amplitude spikes arise very rarely (thanks to statistical averaging) so that by applying a specific processing (no coding) only on DMT signals whose amplitudes exceed a given amplitude A_{Clip}, one can obtain a DMT symbol stream with almost no amplitudes exceeding A_{Clip}.

The paper is organized as follows. Section II presents the basics of the proposed method. In Section III, the resulting improvement of system performance in terms of signal-to-noise ratio (SNR) is derived. Conclusions are reported in Section IV.

II. The Proposed Method

The basic idea behind the proposed method can be described as follows. Assume that the maximum amplitude of the clipped DMT signal, A_{Clip}, is chosen so that the probability of amplitude clipping is lower than a specified value. In the DMT transmitter, the symbols generated by the IFFT are analyzed by a peak detector which provides an indication of the presence or absence of amplitude clipping. According to this indication, two distinct actions are taken:

Case a: If the amplitude of the DMT symbol never exceeds A_{Clip}, then the symbol is sent to the transmitter front-end without any change.

Case b: If the generated DMT symbol has at least one sample whose amplitude exceeds A_{Clip}, then it is not passed directly to the transmitter front-end. Instead, the phasor of each QAM-modulated carrier is changed by means of a fixed phasor-transformation and a new DMT symbol is generated by the IFFT. By careful selection of the phasor-transformation, the probability of clipping this new symbol (second pass) will be very low. (The resulting overall clipping probability will be calculated later on.)

Paper approved by S. Benedetto, the Editor for Signal Design, Modulation, and Detection of the IEEE Communications Society. Manuscript received March 31, 1995; revised September 11, 1995.

The authors are with the Alcatel Corporate Research Center, Antwerp, B-2018 Belgium.

Publisher Item Identifier S 0090-6778(96)07387-4.

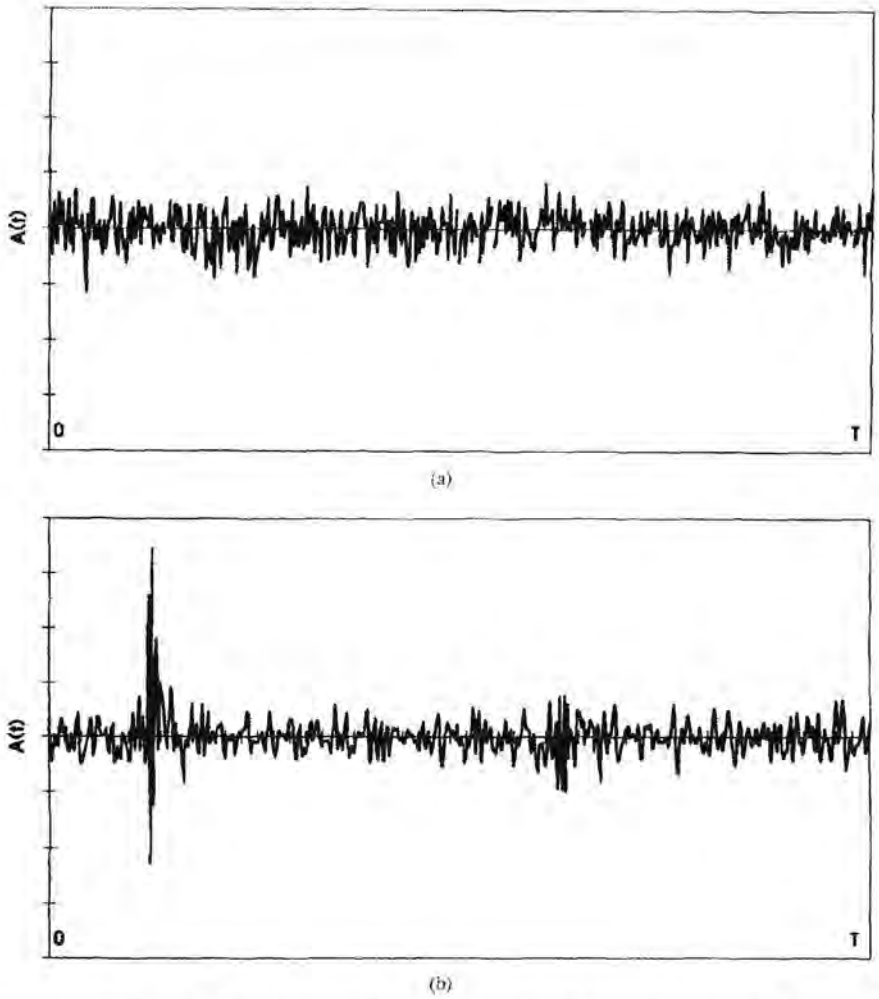

Fig. 1. Instantaneous amplitude $A(t)$ of two DMT symbols generated with two distinct sets of phasors $\{r_m^k\}_1$ and $\{r_m^k\}_2$, and $N = 256$.

The receiver at the far-end is informed about the application (or not) of the phasor-transformation at the transmitter, and applies the inverse transformation (Case b) or not (Case a) after demapping the QAM-modulated carriers. This extra information requires only one bit per DMT symbol. This bit could be provided by modulation of the pilot tone that otherwise carries no information and that is permanently used to maintain synchronization. Forward error correction coding and/or duplication of this information over another or several tones can be envisaged to improve the reliability of this data recovery.

Many phasor-transformations can be used. An easy-to-implement fixed random phasor transformation (known at the receiver) will be considered in what follows. Several other (more involved) transformations can be used as well without affecting the main results presented here.

The overall probability of clipping with the "two-pass" method described above can readily be obtained using (2). The probability that a given sample in the DMT symbol has an absolute amplitude larger than A_{Clip} ($A_{\text{Clip}} > 0$) is simply given by

$$P = 2 \cdot \int_{A_{\text{Clip}}}^{+\infty} p(x)\, dx = 1 - \text{erf}\left(\frac{A_{\text{Clip}}}{\sqrt{2} \cdot \sigma}\right) \tag{3}$$

where $\text{erf}(t)$ is the error function defined by

$$\text{erf}(t) = \frac{2}{\sqrt{\pi}} \cdot \int_0^t e^{-y^2}\, dy \cong 1 - \frac{e^{-t^2}}{t\sqrt{\pi}} \cdot \left[1 - \frac{1}{2t^2}\right].$$

Assuming $2N$ independent samples per DMT symbol, the probability that the symbol must be clipped after the first pass (i.e., at least one sample has an absolute amplitude larger than A_{Clip}) is given by

$$P_{\text{Clip}/1} = 1 - (1 - P)^{2N}. \tag{4}$$

The validity of (4) has been confirmed with great accuracy (better than 1%) by extensive computer simulations.

We assume that due to the random phasor-transform (with large N), the probability that the symbol must be clipped after the second-pass, $P_{\text{Clip}/2}$, is equal to $P_{\text{Clip}/1}$. This is particularly the case if the transformation is a random bijection

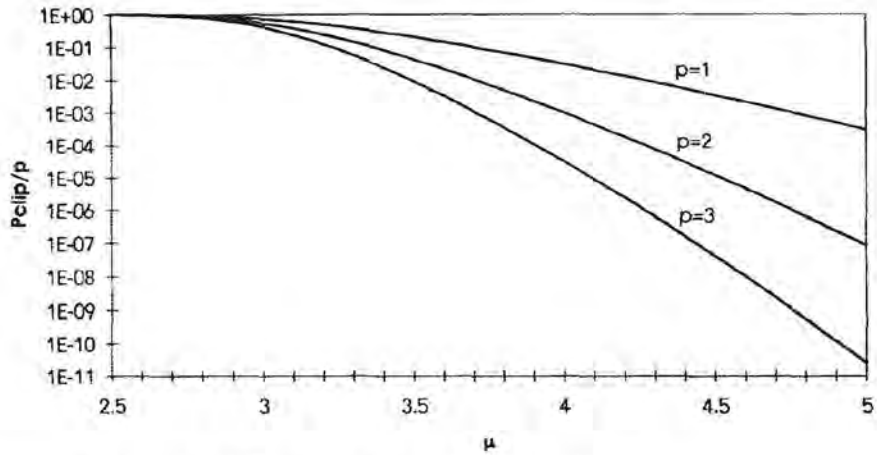

Fig. 2. Probability of clipping the transmitted DMT signal as a function of μ for $p = 1, 2, and 3$.

on the set of constellation points. This means that the sets of constellation points belonging to the sub-ensemble of clipped symbols are equiprobably transformed into the whole ensemble of DMT symbols. As the decision is taken after the first pass, only clipped symbols are submitted to a second pass, so that the overall clipping probability is given by

$$P_{\text{Clip/Total}} = P_{\text{Clip/1}} \cdot P_{\text{Clip/2}} = P^2_{\text{Clip/1}}. \tag{5}$$

Again, extensive computer simulations have been carried out to confirm the validity of (5).

Defining the dimensionless parameter $\mu = A_{\text{Clip}}/\sigma$ and making use of (3), (4), and (5), we obtain

$$P_{\text{Clip/Total}} = \left[1 - \text{erf}^{2N}\left(\frac{\mu}{\sqrt{2}}\right)\right]^2. \tag{6}$$

In general, for a p-pass method, the overall probability of clipping is given by $P_{\text{Clip/Total}} = P^p_{\text{Clip/1}}$, which tends rapidly to zero as p increases.

In practice, the number of passes (p) is limited by the speed of the IFFT at the transmitter. It is noteworthy, however, that e.g. the 2-pass method does not necessarily require a factor of 2 increase of the (I)FFT speed. Indeed, since the probability of clipping after the first pass is low, say less than 10^{-2}, the speed of the IFFT should only be increased by a few percent provided that a DMT symbol buffer is used to absorb the delay incurred by the second pass.

Note also that for $p > 2$, the method requires the transmission of $\log_2 p$ b to inform the far-end receiver about the number of passes that have been applied to generate the DMT symbol. In practice, this additional control information is negligible compared to the data rate.

Fig. 2 represents the clipping probability for the 1-pass, 2-pass, and 3-pass methods as a function of μ. For example, with $\mu = 4$ the 2-pass and the 3-pass methods reduce the probability of clipping down to 10^{-3} and less than 3.10^{-5}, respectively.

III. Performance Improvements

The system performance can be expressed in terms of the SNR for $p = 0$ (i.e., no clipping) and $\phi \geq 1$. In this section, we will restrict ourselves to the cases $p = 0, 1$, and 2 . Extension of the present analysis to the case where $p > 2$ is straightforward.

We consider an additive white Gaussian noise (AWGN) channel. Different noise sources will contribute to the overall SNR: a) at the transmitter: the clipping noise (only for $p =$ 1 or 2) and the quantization noise of the D/A convertor, and b) at the receiver; the AWGN and the quantization noise of the A/D convertor.

We will assume a resolution of b b for the D/A and A/D convertors, and a quantization noise for $p = 0$ that is a factor α lower than the AWGN. Therefore, without clipping ($p = 0$), the quantization noise of the D/A and A/D convertors and the AWGN are, respectively, given by

$$Q_0 = \frac{(2A_{\max})^2}{12.2^{2b}} \tag{7}$$

$$\text{AWGN} = \alpha \cdot Q_0 \tag{8}$$

and where $A_{\max}$ is the maximum amplitude of the DMT symbols. $A_{\max}$ can be expressed as a function of the signal power σ^2 and the crest factor ν: $A_{\max} = \nu \cdot \sigma$. The crest factor is fixed by N and the QAM constellation size according to [6]

$$\nu = \frac{1+\sqrt{2}}{2} \cdot \sqrt{3N} \cdot \sqrt{\frac{L-1}{L+1}} \tag{9}$$

where L^2 is the QAM constellation size (e.g., $L = 4$ for 16-QAM).

When clipping is applied ($p = 1$ or 2), the quantization noise becomes

$$Q_{\text{Clip}} = \frac{(2A_{\text{Clip}})^2}{12.2^{2b}}. \tag{10}$$

The noise due to clipping has been derived in [6] for $p = 1$ and is rewritten here for convenience

$$N_{\text{Clip/1}} = 2 \cdot \int_{A_{\text{Clip}}}^{+\infty} (x - A_{\text{Clip}})^2 \cdot p(x)\, dx = \sigma^2$$

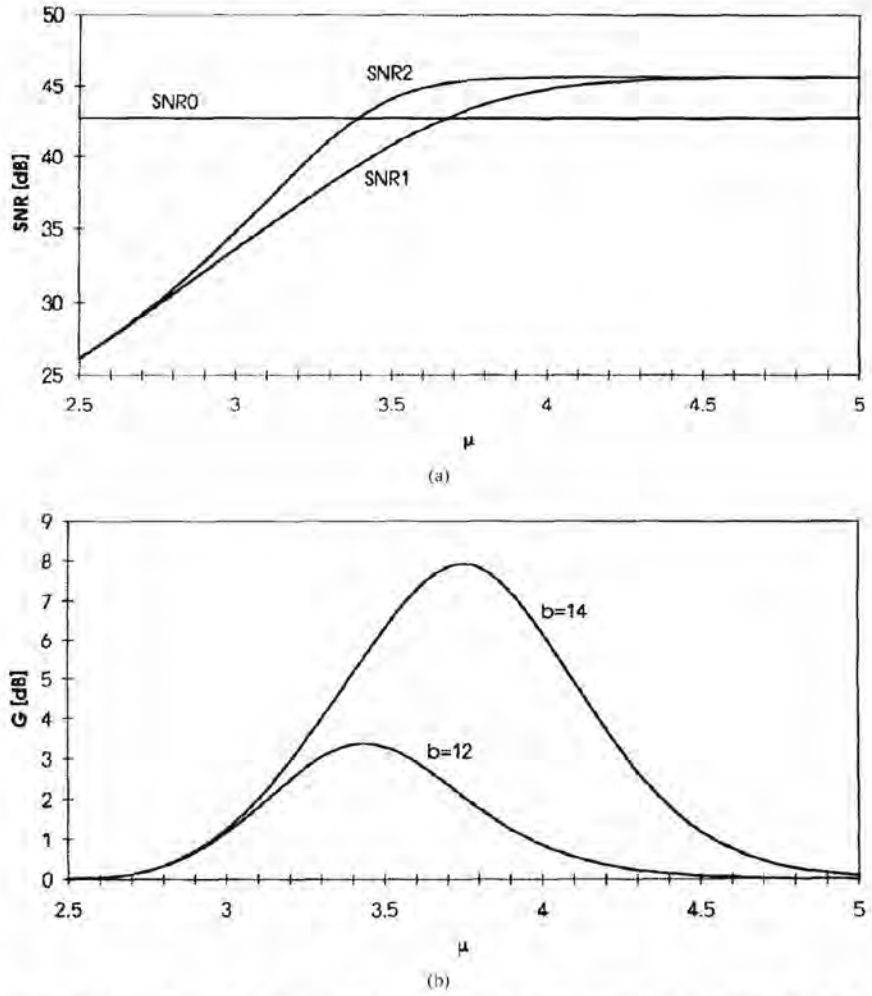

Fig. 3. (a) The SNR's (in dB) for $p = 0$ (no clipping), $p = 1$ and $p = 2$ as a function of μ for $a = 2, b = 12$ and (b) the gain G (in dB) as a function of μ for $a = 2, b = 12$ and $b = 14$.

$$\cdot \left\{ (1+\mu^2) \cdot \operatorname{erfc}\left(\frac{\mu}{\sqrt{2}}\right) - \sqrt{\frac{2}{\pi}} \cdot \mu \cdot e^{-(\mu^2/2)} \right\} \tag{11}$$

where $\operatorname{erfc}(t) = 1 - \operatorname{erf}(t)$.

In order to calculate the clipping noise for $p = 2$, we first need to determine the pdf of $A(t)$ for $|A| > A_{\text{Clip}}$, and then follow the same reasoning as in [6]. This pdf is readily obtained as

$$p'(x) = P_{\text{Clip}/1} \cdot p(x) \quad \text{for} \quad |x| > A_{\text{Clip}} \tag{12}$$

where $p(x)$ and $P_{\text{Clip}/1}$ are given by (2) and (4), respectively.

Therefore, the total power of the clipped portion of the DMT symbols for $p = 2$ is given by

$$N_{\text{Clip}/2} = 2 \cdot \int_{A_{\text{Clip}}}^{+\infty} (x - A_{\text{Clip}})^2 \cdot p'(x)\, dx = P_{\text{Clip}/1} \cdot N_{\text{Clip}/1}. \tag{13}$$

Making use of $A_{\max}/A_{\text{Clip}} = \nu/\mu$, the overall noise for $p = 0$, 1 and 2 can be expressed as

$$N_{p=0} = 2 \cdot Q_0 + \text{AWGN} = (2+\alpha) \cdot Q_0 \tag{14.a}$$

$$N_{p=1} = 2 \cdot Q_{\text{Clip}} + \text{AWGN} + N_{\text{Clip}/1} = \left[2\left(\frac{\mu}{\nu}\right)^2 + \alpha \right] \cdot Q_0 + N_{\text{Clip}/1} \tag{14.b}$$

$$N_{p=2} = 2 \cdot Q_{\text{Clip}} + \text{AWGN} + N_{\text{Clip}/2} = \left[2\left(\frac{\mu}{\nu}\right)^2 + \alpha \right] \cdot Q_0 + N_{\text{Clip}/2}. \tag{14.c}$$

(The factor 2 in the right-hand side of (14) is due to the quantization noise of the D/A at the transmitter and the quantization noise of the A/D at the receiver.)

The associated SNR's are obtained using (3), (4), (7), (11), (13), and (14) and their closed-form expressions are given by

$$\text{SNR}_{p=0} = \frac{3.2^{2b}}{(2+\alpha) \cdot \nu^2} \tag{15.a}$$

$$\text{SNR}_{p=1} = \left\{ \left[2\left(\frac{\mu}{\nu}\right)^2 + \alpha \right] \cdot \left(\frac{\nu^2}{3.2^{2b}} \right) + \left[(1+\mu^2) \cdot \operatorname{erfc}\left(\frac{\mu}{\sqrt{2}}\right) \right.$$

$$- \sqrt{\frac{2}{\pi}} \cdot \mu \cdot e^{-(\mu^2/2)} \Bigg] \Bigg\}^{-1} \quad (15.b)$$

$$\mathrm{SNR}_{p=2} = \left\{ \left[2\left(\frac{\mu}{\nu}\right)^2 + \alpha \right] \cdot \left(\frac{\nu^2}{3.2^{2b}}\right) + \left(1 - \mathrm{erf}^{2N}\left(\frac{\mu}{\sqrt{2}}\right)\right) \cdot \left[(1+\mu^2) \cdot \mathrm{erfc}\left(\frac{\mu}{\sqrt{2}}\right) - \sqrt{\frac{2}{\pi}} \cdot \mu \cdot e^{-(\mu^2/2)} \right] \right\}^{-1}. \quad (15.c)$$

The SNR's (in dB) for $p = 0, 1$, and 2 derived from (15) are plotted in Fig. 3(a) as a function of μ for $\alpha = 2$, $b = 12$ b and $\nu = 25.9$ [(9) with $L = 4$ and $N = 256$]. It is seen that, as compared with the $p = 0$ case, an improvement in SNR is obtained provided that $\mu \geq 3.7$ for $p = 1$ and $\mu \geq 3.4$ for $p = 2$. This improvement in SNR can be used at profit to reduce the required resolution of the D/A-A/D convertors as discussed in [6].

The system performance improvement provided by the proposed method ($p = 2$) in comparison with $p = 1$ can be characterized by the gain G in SNR: $G = \mathrm{SNR}_{p=2}/\mathrm{SNR}_{p=1}$.

Fig. 3(b) shows the gain G (in dB) as a function of μ for $\alpha = 2$, $b = 12$ and $b = 14$. It is seen that G is bell-shaped and that its maximum value increases with b. The maximum gain is 3.4 dB for $b = 12$ and is as high as 7.9 dB for $b = 14$. Notice that for $p = 2$ the relevant values of G are only those associated with the values of μ that satisfy the condition $\mathrm{SNR}_{p=2} \geq \mathrm{SNR}_{p=0}$. Fortunately, for a given b, the value of μ that provides the maximum gain G is very close to the value of μ that satisfies the condition $\mathrm{SNR}_{p=2} = \mathrm{SNR}_{p=0}$.

IV. Conclusion

A method to decrease the probability of clipping DMT symbols by several orders of magnitude has been described. The method does not use any kind of pre-coding and hence, does not increase the actual transmission data rate. Significant improvements in SNR of about 3 dB up to 8 dB as compared to the case or brute force clipping can be achieved. This can be used at profit to reduce the required resolution of the D/A-A/D convertors, to decrease the maximum amplitude of the transmitted signal, or to provide an extra signal-to-noise margin of the communication system.

Acknowledgment

The authors are very grateful to J.-F. Van Kerckhove for his computer simulations that have confirmed the validity of (4) and (5). They also wish to thank the reviewers for their detailed and valuable comments.

References

[1] J. A. C. Bingham, "Multicarrier modulation for data transmission: an idea whose time has come," *IEEE Commun. Mag.*, pp. 5–14, May 1990.
[2] R. Lassalle *et al.*, "Principles of modulation and channel coding for digital audio broadcasting for mobile receivers," *EBU Technol. Rev.*, pp. 168–190, 1987.
[3] T. de Couasnon *et al.*, "OFDM for digital TV broadcasting," *Signal Processing*, vol. 39, pp. 1–32, Sept. 1994.
[4] A. Ruiz *et al.*, "Discrete multiple tone modulation with Coset coding for the spectrally shaped channel," *IEEE Trans. Commun.*, vol. 40, no. 6, pp. 1012–1029, June 1992.
[5] Draft American National Standard for Telecommunications—Network and Customer Installation Interfaces, "Asymmetric digital subscriber line (ADSL) metallic interface," T1E1.4/94-007R7, Sept. 1994.
[6] D. J. G. Mestdagh *et al.*, "Effect of amplitude clipping in DMT-ADSL transceivers," *Electron. Lett.*, vol. 29, no. 15, pp. 1354–1355, July 1993. See also, D. J. G. Mestdagh *et al.*, "Analysis of clipping effect in DMT-based ADSL systems," in *Proc. IEEE Int. Conf. Commun. ICC'94*, May 1–5, 1994, pp. 293–300.
[7] Richard Gross *et al.*, "SNR and spectral properties for a clipped DMT ADSL signal," in *Proc. IEEE Int. Conf. Commun., ICC'94*, May 1–5, 1994, pp. 843–847.
[8] A. E. Jones *et al.*, "Block coding scheme for reduction of peak to mean envelope power ratio of multicarrier transmission schemes," *IEE Electron. Lett.*, vol. 30, no. 25, pp. 2098–2099, Dec. 1994. See also, T. A. Wilkinson and A. E. Jones, "Minimization of the peak to mean envelope power ratio of multicarrier transmission schemes by block coding," *IEEE 45th Veh. Technol. Conf.*, Chicago, 1995, pp. 825–829.
[9] S. J. Shepherd *et al.*, "Simple coding scheme to reduce the peak factor in QPSK multicarrier modulation," *Electron. Lett.*, vol. 31, no.14, pp. 1131–1132, July 1995.

A COMPARISON OF PEAK POWER REDUCTION SCHEMES FOR OFDM

Stefan H. Müller and Johannes B. Huber

Lehrstuhl für Nachrichtentechnik, Universität Erlangen-Nürnberg
Cauerstraße 7, D-91058 Erlangen, Germany
e-mail: *smueller@nt.e-technik.uni-erlangen.de*, WWW: *http://www-nt.e-technik.uni-erlangen.de/~dcg*

Abstract — Two powerful and distortionless peak power reduction schemes for Orthogonal Frequency Division Multiplexing (OFDM) are compared. One investigated technique is selected mapping (SLM) where the actual transmit signal is selected from a set of signals and the second scheme utilizes phase rotated partial transmit sequences (PTS) to construct the transmit signal. Both approaches are very flexible as they do not impose any restriction on the modulation applied in the subcarriers or on their number. They both introduce some additional system complexity but nearly vanishing redundancy to achieve markedly improved statistics of the multicarrier transmit signal. The schemes are compared by simulation results with respect to the required system complexity and transmit signal redundancy.

1. INTRODUCTION

Besides a lot of advantages, some drawbacks become apparent, when using OFDM in transmission systems. A major obstacle is that the multiplex signal exhibits a very high peak–to–average power ratio (PAR). Therefore, nonlinearities may get overloaded by high signal peaks, causing intermodulation among subcarriers and — more critical — undesired out–of–band radiation. If RF power amplifiers are operated without large power back–offs, it is impossible to keep the out–of–band power below specified limits. This leads to very inefficient amplification and expensive transmitters so that it is highly desirable to reduce the PAR. A variety of methods for that purpose is proposed in literature (e.g. [4, 10, 3]).

Here, we concentrate on two recently proposed flexible and distortionless methods for the reduction of the PAR by way of introducing little redundancy. The SLM method [1, 2] (similar methods are described in [9, 5]) is compared to the PTS approach [8, 7]. In SLM the transmitter selects one favorable transmit signal from a set of sufficiently different signals which all represent the same information, while in PTS the transmitter constructs its transmit signal with low PAR by coordinated addition of appropriately phase rotated signal parts.

Section 2 recapitulates OFDM signaling. In Section 3 we report statistical characteristics of the OFDM transmit signal. The two investigated PAR reduction schemes are looked at again in Section 4. Simulation results to compare their performance are presented in Section 5. There, the PAR reduction capability of both schemes is set against the theoretical limit of achievable minimum PAR versus redundancy and we will find that they are considerably near this limit.

0-7803-4198-8/97/$10.00 © 1997 IEEE

2. OFDM TRANSMISSION

The idea of OFDM is to use D_u separate subcarriers, having a uniform frequency spacing. The frequency multiplexing is implemented by using the inverse discrete Fourier transform (IDFT) for D–ary ($D \geq D_u$) vectors in the modulator.

At first, binary data is mapped onto D_u carriers. Thereby, subcarrier ν of OFDM symbol interval μ is modulated with the complex coefficient $A_{\mu,\nu}$. Here, we assume that in all D_u active carriers the same complex–valued zero–mean signal set $\mathcal{A}$ with variance $\sigma_{\mathcal{A}}^2$ is used, but the results can easily be extended to mixed signal constellations. Inactive carriers are set to zero in order to shape the power density spectrum of the transmit signal appropriately.

The *subcarrier vector* $\mathbf{A}_\mu = [A_{\mu,0}, \ldots, A_{\mu,D-1}]$ comprising all carrier amplitudes associated with OFDM symbol interval μ is transformed into time domain, using a D–point IDFT. This results in the T–spaced discrete–time representation of the transmit signal in the μ–th block, given by $\mathbf{a}_\mu = [a_{\mu,0}, \ldots, a_{\mu,D-1}]$ with $a_{\mu,\rho} = \frac{1}{\sqrt{D}} \sum_{\nu=0}^{D-1} A_{\mu,\nu} \cdot \mathrm{e}^{+\mathrm{j}\frac{2\pi}{D}\nu\rho}$, $0 \leq \rho < D$. In the following $\mathbf{a}_\mu = \mathrm{IDFT}\{\mathbf{A}_\mu\}$ denotes this transform relationship. Here, the modulation period T is related with the symbol period T_s in each subcarrier by $T_s = D \cdot T$.

Finally, the samples $a_{\mu,\rho}$ are transmitted using ordinary T–spaced pulse amplitude modulation. The guard interval usually introduced before transmission consists of a partial repetition of some $a_{\mu,\rho}$ and therefore does not affect the PAR. Thus, it is not considered here.

For what follows we coin the term *transmit sequence* for $\mathbf{a}_\mu$. The peak power optimized alternative transmit sequence will be denoted as $\tilde{\mathbf{a}}_\mu$.

3. TRANSMIT SEQUENCE STATISTICS

Clearly, the power amplifier has to deal with the continuous–time transmit signal after a specific impulse shaping. For simplicity, we will only focus on the PAR of the underlying T–spaced sampled representation $\mathbf{a}_\mu$ of this signal. Under certain circumstances and depending on the steepness of the impulse–shaping filter's frequency response in the transition region (length of impulse response), special attention has to be dedicated to the continuous–time behaviour, too.

3.1. STATISTICAL PROPERTIES

We define a discrete–time PAR associated with OFDM symbol interval μ as

$$\chi_\mu \stackrel{\text{def}}{=} \max_{0 \leq \rho < D} |a_{\mu,\rho}|^2 \Big/ \mathcal{E}\left\{|a_{\mu,\rho}|^2\right\}, \qquad (1)$$

where $\mathcal{E}\{\cdot\}$ denotes expectation. Due to Parseval's theorem the average power of the transmit sequences is $\sigma_a^2 \stackrel{\text{def}}{=} \mathcal{E}\left\{|a_{\mu,\rho}|^2\right\} = \frac{D_u}{D} \cdot \sigma_A^2$.

Applying the central limit theorem, while assuming that D_u is sufficiently large (≥ 64 is sufficient), the $a_{\mu,\rho}$ are zero-mean complex-valued near Gaussian distributed random variables with variance σ_a^2.

Introducing the OFDM transmit signal magnitude $u = |a_{\mu,\rho}| \geq 0$, we obtain (independent from D) the Rayleigh density

$$p_u(u) = \frac{2u}{\sigma_a^2} \cdot \mathrm{e}^{-u^2/\sigma_a^2} \cdot \delta_{-1}(u) \tag{2}$$

for the probability density function (pdf) of u (cf. Fig. 4). Clearly, $\delta_{-1}(u)$ in Eq. (2) denotes the unit step function.

Following the exposition in [2, 5, 6], the probability that χ_μ of a randomly generated D-carrier OFDM symbol exceeds the PAR threshold $\chi_0 = a_0^2/\sigma_a^2$ can be approximated by (cf. Fig. 3)

$$\Pr\{\chi_\mu > \chi_0\} = 1 - \left(1 - \mathrm{e}^{-\chi_0}\right)^D. \tag{3}$$

Note that the latter expression does not depend on the PAR of the signal set $\mathcal{A}$ used in the subcarriers.

3.2. THEORETICAL LIMIT FOR MINIMUM PAR

The ideal distortionless PAR reduction scheme introduces redundancy to exclude "bad" OFDM symbols from transmission. Ideally, R_{ap} ("antipeak") bits per symbol allow to reject the larger fraction of $\left(1 - 2^{-R_{\text{ap}}}\right)$ from the entire set of possible OFDM symbols [6]. If e.g. $\Pr\{\chi_\mu > \chi_0\} = \frac{3}{4}$, then $\frac{1}{4}$ of the entire set of possibly generated OFDM symbols have a PAR lower than χ_0. Clearly, only $R_{\text{ap}} = 2$ bits per symbol are required to distinguish these favorable OFDM symbols from the undesired rest. Therefore, $1 - 2^{-R_{\text{ap}}} = \Pr\{\chi_\mu > \chi_0\}$ gives the relation between redundancy R_{ap} and the theoretically achievable minimum PAR χ_0. Incorporating Eq. (3) and solving for χ_0 yields

$$\chi_0 = -\ln\left(1 - 2^{-\frac{R_{\text{ap}}}{D}}\right), \tag{4}$$

which represents the lower bound for χ_0 when R_{ap} bits redundancy are distributed on D carriers, no matter which modulation is used in them (cf. Fig. 5).

In the following section two generally related methods are recapitulated which both spread the redundancy appropriately over the entire OFDM symbol. These two schemes do not result in an inflexible joint coding and modulation scheme as in [4, 10] and furthermore they are effective with an arbitrarily large number of subcarriers.

4. REDUCING PEAK POWER IN OFDM

4.1. SELECTED MAPPING

In this most general approach [1, 2] it is assumed that U statistically independent alternative transmit sequences $\mathbf{a}_\mu^{(u)}$ represent the same information. Then, that sequence $\tilde{\mathbf{a}}_\mu = \mathbf{a}_\mu^{(\tilde{u}_\mu)}$ with the lowest PAR, denoted as $\tilde{\chi}_\mu$, is selected for transmission. The probability that $\tilde{\chi}_\mu$ exceeds χ_0 is approximated by [2, 5]

$$\Pr\{\tilde{\chi}_\mu > \chi_0\} = \left(1 - \left(1 - \mathrm{e}^{-\chi_0}\right)^D\right)^U. \tag{5}$$

Because of the selected assignment of binary data to the transmit signal, this principle is called selected mapping in [2, 6].

A set of U markedly different, distinct, pseudo-random but fixed vectors $\mathbf{P}^{(u)} = [P_0^{(u)}, \ldots, P_{D-1}^{(u)}]$, with $P_\nu^{(u)} = \mathrm{e}^{+\mathrm{j}\varphi_\nu^{(u)}}$, $\varphi_\nu^{(u)} \in [0, 2\pi)$, $0 \leq \nu < D$, $1 \leq u \leq U$ must be defined. The subcarrier vector $\mathbf{A}_\mu$ is multiplied subcarrier-wise with each one of the U vectors $\mathbf{P}^{(u)}$, resulting in a set of U different subcarrier vectors $\mathbf{A}_\mu^{(u)}$ with components

$$A_{\mu,\nu}^{(u)} = A_{\mu,\nu} \cdot P_\nu^{(u)}, \quad 0 \leq \nu < D, \quad 1 \leq u \leq U. \tag{6}$$

Then, all U alternative subcarrier vectors are transformed into time domain to get $\mathbf{a}_\mu^{(u)} = \text{IDFT}\left\{\mathbf{A}_\mu^{(u)}\right\}$ and finally that transmit sequence $\tilde{\mathbf{a}}_\mu = \mathbf{a}_\mu^{(\tilde{u}_\mu)}$ with the lowest PAR $\tilde{\chi}_\mu$ is chosen. The SLM-OFDM transmitter is depicted in Fig. 1, where it is visualized that one of the alternative subcarrier vectors can be the unchanged original one.

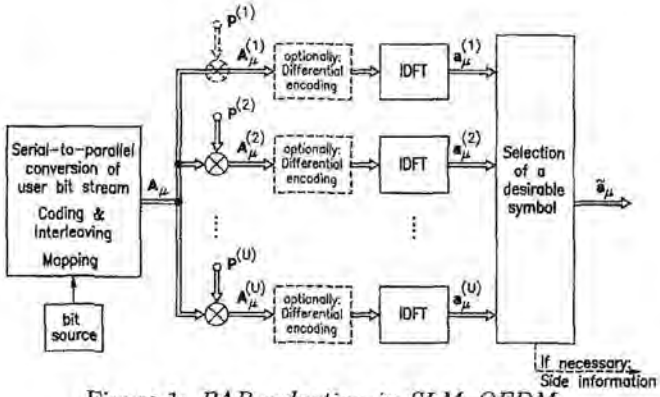

Figure 1: *PAR reduction in SLM-OFDM.*

Optionally, differentially encoded modulation may be applied before the IDFT and right after generating the alternative OFDM symbols. At the receiver, differential demodulation has to be implemented right after the DFT.

4.2. PARTIAL TRANSMIT SEQUENCES

In this scheme [8, 7] the subcarrier vector $\mathbf{A}_\mu$ is partitioned into V pairwise disjoint subblocks $\mathbf{A}_\mu^{(v)}$, $1 \leq v \leq V$. All subcarrier positions in $\mathbf{A}_\mu^{(v)}$, which are already represented in another subblock are set to zero, so that $\mathbf{A}_\mu = \sum_{v=1}^{V} \mathbf{A}_\mu^{(v)}$. We introduce complex-valued rotation factors $b_\mu^{(v)} = \mathrm{e}^{+\mathrm{j}\varphi_\mu^{(v)}}$, $\varphi_\mu^{(v)} \in [0, 2\pi)$, $1 \leq v \leq V$, $\forall \mu$, enabling a modified subcarrier vector

$$\tilde{\mathbf{A}}_\mu = \sum_{v=1}^{V} b_\mu^{(v)} \cdot \mathbf{A}_\mu^{(v)}, \tag{7}$$

which represents the same information as $\mathbf{A}_\mu$, if the set $\left\{b_\mu^{(v)}, 1 \le v \le V\right\}$ (as side information) is known for each μ. Clearly, simply a joint rotation of all subcarriers in subblock v by the same angle $\varphi_\mu^{(v)} = \arg\left(b_\mu^{(v)}\right)$ is performed.

To calculate $\tilde{\mathbf{a}}_\mu = \text{IDFT}\left\{\tilde{\mathbf{A}}_\mu\right\}$, the linearity of the IDFT is exploited. Accordingly, the subblocks are transformed by V separate and parallel D-point IDFTs, yielding

$$\tilde{\mathbf{a}}_\mu = \sum_{v=1}^{V} b_\mu^{(v)} \cdot \text{IDFT}\left\{\mathbf{A}_\mu^{(v)}\right\} = \sum_{v=1}^{V} b_\mu^{(v)} \cdot \mathbf{a}_\mu^{(v)}, \qquad (8)$$

where the V so-called partial transmit sequences $\mathbf{a}_\mu^{(v)} = \text{IDFT}\left\{\mathbf{A}_\mu^{(v)}\right\}$ have been introduced. Based on them a peak value optimization is performed by suitably choosing the free parameters $b_\mu^{(v)}$ such that the PAR is minimized for $\tilde{b}_\mu^{(v)}$. The $b_\mu^{(v)}$ may be chosen with continuous-valued phase angle, but more appropriate in practical systems is a restriction on a finite set of W (e.g. 4) allowed phase angles.

The optimum transmit sequence then is

$$\tilde{\mathbf{a}}_\mu = \sum_{v=1}^{V} \tilde{b}_\mu^{(v)} \cdot \mathbf{a}_\mu^{(v)}. \qquad (9)$$

The PTS-OFDM transmitter is depicted in Fig. 2 with the hint, that one PTS can always be left unrotated.

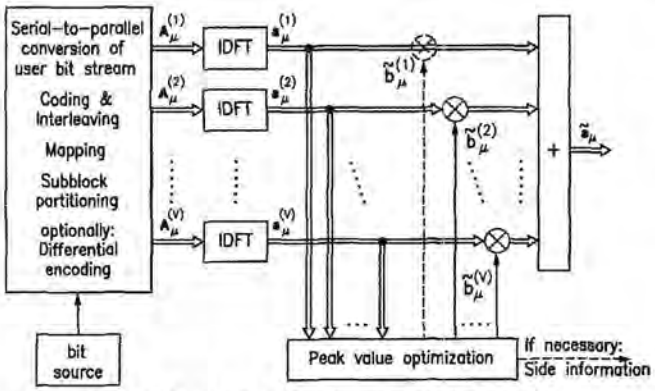

Figure 2: *PAR reduction in PTS-OFDM.*

We refer to [8, 6] for the discussion of an advantageous application of PTS employing differentially encoded modulation across subcarriers (i.e. in direction of frequency).

So far, no specific assignment of subcarriers to subblocks (subblock partitioning) has been given, but it has considerable influence on the PAR reduction capability of PTS. This topic is discussed in [7], where a pseudo-random (but still disjoint) subblock partitioning has been found to be the best choice for high PAR reduction.

It should be noted, that PTS can be interpreted as a structurally modified special case of SLM, if $W^{V-1} = U$ and the $\mathbf{P}^{(u)}$ are chosen in accordance with the PTS partitioning and all the allowed rotation angle combinations $\{b_\mu^{(v)}\}$. But with this construction rule, especially for a large number of vectors $\mathbf{P}^{(u)}$, their statistical independence is usually no longer satisfied, so that Eq. (5) does not hold any longer.

4.3. *REDUNDANCY (SIDE INFORMATION)*

Both schemes require, that the receiver has knowledge about the generation of the transmitted OFDM signal in symbol period μ. Thus, in PTS the set with all rotation factors $\tilde{b}_\mu^{(v)}$ and in SLM the number $\tilde{u}_\mu$ of the selected $\mathbf{P}^{(\tilde{u}_\mu)}$ has to be transmitted to the receiver unambiguously so that this one can derotate the subcarriers appropriately. The number of bits required for canonical representation of this side information is the redundancy R_{ap} introduced by the PAR reduction scheme with PTS and SLM. As this side information is of highest importance to recover the data, it should be carefully protected by channel coding, but the hereby introduced additional redundancy is not considered here.

In PTS the number of admitted combinations of rotation angles $\{b_\mu^{(v)}\}$ should not be excessively high, to keep the explicitely transmitted side information within a reasonable limit. If in PTS each $b_\mu^{(v)}$ is exclusively chosen from a set of W admitted angles, then $R_{\text{ap}} = (V-1)\log_2 W$ bits per OFDM symbol are needed for this purpose. In SLM $R_{\text{ap}} = \log_2 U$ bits are required for side information.

Both schemes use the introduced redundancy to synthesize alternative signal representations, which all have to be checked for PAR. Clearly, their number is given by $2^{R_{\text{ap}}}$. In SLM this value is U while in PTS we obtain W^{V-1} alternatives, a number which can get very high.

In PTS the choice $b_\mu^{(v)} \in \{\pm 1, \pm \text{j}\}$ ($W = 4$) is very interesting for an efficient implementation, as actually no multiplication must be performed, when rotating and combining the PTSs $\mathbf{a}_\mu^{(v)}$ to the peak-optimized transmit sequence $\tilde{\mathbf{a}}_\mu$ in Eq. (9). For SLM, choosing $P_\nu^{(u)}$ from the latter set has the same advantage, when generating the alternative subcarrier vectors by applying Eq. (6).

5. COMPARATIVE SIMULATION RESULTS

The presented simulations were performed with $D_{\text{u}} = D = 128$ carriers modulated with 16QAM. The statistics of peak and instantaneous power in randomly generated OFDM symbols have been investigated.

In PTS, an optimum pseudo-random [7] disjoint assignment of $\approx D/V$ subcarriers to each subblock is used. Here, the optimum $\tilde{b}_\mu^{(v)}$ are found by an exhaustive search over all combinations of rotation angles. For SLM, U statistically independent rotation vectors $\mathbf{P}^{(u)}$ are used. The rotation vectors are actually obtained from random binary sequences mapped on 4PSK symbols. In Fig. 3 simulation results for $\Pr\{\chi_\mu > \chi_0\}$ achieved with V PTS-subblocks, where each $b_\mu^{(v)}$ is chosen from a 4PSK-constellation ($W = 4$) are set against SLM-OFDM with U alternative subcarrier vectors. Note that $V = U$ IDFTs are needed in either scheme but PTS will usually provide a greater multiplicity of signal representations to be checked for PAR. The simulated characteristic of original OFDM and the theoretical expression from Eq. (3) are plotted there as well and theory corresponds well with the simulation result. It follows from this diagram that PTS with $W = 4$ rotations and $V = 2$ IDFTs (and therefore 4 signal

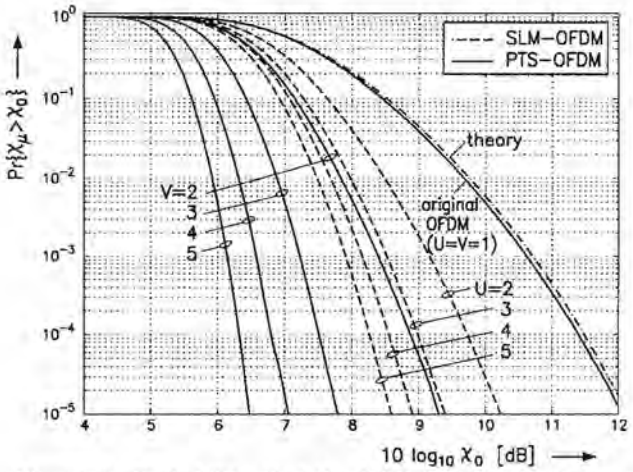

Figure 3: *Probability that the PAR of a randomly generated 128–carrier OFDM transmit sequence exceeds χ_0 for U IDFTs in SLM and V IDFTs in PTS with $W = 4$.*

representations) achieves a slightly better performance than SLM with $U = 3$ IDFTs (3 signal representations). The gap would get even larger if W is further increased in PTS (W signal representations, if $V = 2$). Generally, PTS outperforms SLM in PAR reduction, if the number of IDFTs is fixed, but clearly with more alternative signals to be processed.

As already mentioned 16QAM modulation (PAR of $\mathcal{A}$: 2.55 dB) was used in each of the 128 subcarriers, but theoretically the results do not differ, when using 4PSK modulation (PAR of $\mathcal{A}$: 0 dB). In fact, simulations with 4PSK resulted in minor changes (< 0.1 dB) of *all* depicted PAR statistics.

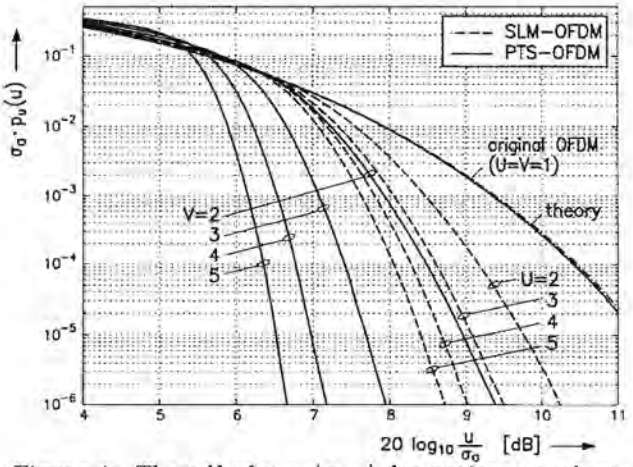

Figure 4: *The pdf of $u = |a_{\mu,\rho}|$ for various numbers of IDFTs in SLM and PTS with $W = 4$ ($D = 128$).*

Fig. 4 shows the pdf of the transmit signal magnitude $u = |a_{\mu,\rho}|$. This is the statistical characteristic, the power amplifier has to cope with. The theoretical expression from Eq. (2) is illustrated additionally and coincides with the simulative result for original OFDM. The benefit of PTS and SLM can be seen from the considerably reduced pdf for high values of the normalized signal magnitude. The slope of the pdf can be adjusted by variation of V and U, respectively.

The effect of PTS and SLM is that both shift probability mass from high amplitude values to lower ones. As PTS is more powerful with the same number of IDFTs, the increase of the pdf around 5 dB is more distinct for PTS.

Table 1 gives a compact overview of PAR reduction capability for SLM set against PTS with various allowed rotation angles, numbers of subblocks and, not considered so far, two different subblock partitionings. The entries provide information about the number of bits R_{ap} for PAR reduction per symbol, and the number of possible signal representations ($2^{R_{ap}}$) enabled by this redundancy. They all have to be checked for PAR, if a selection by exhaustive search is performed. The PAR reduction gain $G_\chi \stackrel{\text{def}}{=} \chi_{\text{original}}/\chi_{\text{reduced}}$ at $\Pr\{\chi_\mu > \chi_0\} = 10^{-5}$ is given in the lower row. The G_χ^a achieved by a PTS subblock partitioning with exclusively adjacent subcarriers [6] is compared to the optimum G_χ^r realizable for pseudo–random subblock partitioning [7]. For PTS, each table entry has to be read like this:

$2^{R_{ap}}$	R_{ap} [bit]
$10\log_{10} G_\chi^a$ [dB]	$10\log_{10} G_\chi^r$ [dB]

.

V,U	2		3		4		5	
PTS	2	1	4	2	8	3	16	4
W=2	1.2	2.0	2.5	3.3	3.4	4.1	4.1	4.7
PTS	4	2	16	4	64	6	256	8
W=4	2.1	3.0	3.6	4.4	4.5	5.2	5.1	5.8
PTS	8	3	64	6	512	9	4k	12
W=8	2.9	3.4	4.2	4.9	5.1	5.8	?	?
PTS	16	4	256	8	4k	12	64k	16
W=16	3.0	3.6	4.2	5.1	?	?	?	?
SLM	2	1	3	1.6	4	2	5	2.3
	2.0		2.8		3.3		3.6	

Table 1: *PAR reduction gain G_χ at $\Pr\{\chi_\mu > \chi_0\} = 10^{-5}$ for PTS–OFDM with V subblocks and W possible rotation angles compared to SLM–OFDM with U alternative subcarrier vectors ($D = 128$).*

Obviously, the pseudo–random assignment of subcarriers to subblocks is 0.5 to 0.9 dB better than the one with exclusively adjacent subcarriers per PTS subblock. The latter is an example for highly structured subblock partitioning, resulting in considerable performance degradation [7].

Note that for some combinations of W and V in PTS an exhaustive optimum search is prohibitive. Table 1 is for 128 carriers and clearly G_χ will be different for other carrier numbers but the tendencies recognizable therein are preserved, especially the fact that for PTS with fixed R_{ap} it is more advantageous to increase V instead of W.

It follows from Table 1 that pseudo–random subblock partitioning in PTS ($W = 2$) with $V = 2$ and 3 performs equivalent to SLM with $U = 2$ and 4, respectively. This shows that for small numbers of W^{V-1} and pseudo–randomized subblock partitioning in PTS, the $\mathbf{P}^{(u)}$ of the equivalent SLM scheme are still statistically independent. This implies that 4 alternative signal representations generated by PTS with 3 IDFTs plus some further vectorial additions achieve the same performance as SLM with 4 IDFTs.

In Fig. 5 the theoretical limit of Eq. (4) is plotted dash–dotted. An ideal method using R_{ap} bits redundancy per symbol can guarantee that no single OFDM symbol ever exceeds χ_0. A distortionless limitation to PAR lower than χ_0 is not possible and this is illustrated as hatched area. Note that the limit derived from a simulated histogram is slightly worse when compared to theory derived from the central limit theorem with all its idealized assumptions.

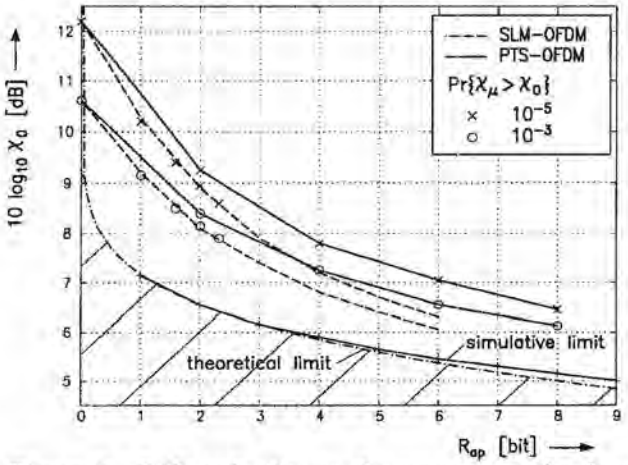

Figure 5: *PAR reduction performance vs. redundancy with respect to the theoretical limit.*

We concentrate on the statistical nature of χ_μ and define $\Pr\{\chi_\mu > \chi_0\} = 10^{-5}$ as unlikely enough not to produce significant out–of–band power after the amplifier. So the "stochastic" PARs occuring with this probability (and 10^{-3} for comparison) are plotted over the number of bits needed for an explicit transmission of side information for pseudo–random subblock partitioning in PTS with $W = 4$ and $V = 1, \ldots, 5$ and SLM with $U = 1, \ldots, 5$. Here, SLM outperforms PTS but clearly on the cost of system complexity. Note that only the marked points on the curve for SLM are simulation results. The dashed curves are derived from Eq. (5), as at $R_{ap} = 6$ an inacceptable high number of 64 IDFTs would be required, compared to only 4 IDFTs plus time–domain optimization in PTS. Given this redundancy, PTS is only 0.8 dB (at 10^{-5}) worse than SLM. For lower R_{ap}, the gap gets even smaller.

6. SUMMARY AND CONCLUSIONS

The paper compared two recently proposed techniques which allow powerful but nonetheless distortionless PAR reduction for OFDM transmission. Both related schemes utilize several IDFTs instead of one and choose (construct) one signal from a multiplicity of (partial) transmit sequences. PTS–OFDM and SLM–OFDM work with arbitrary numbers of subcarriers and types of modulation in them.

In PTS only 1.2% redundancy (cf. Fig. 3, $V = 4$) is needed to reduce the discrete–time PAR by 5.2 dB at $\Pr\{\chi_\mu > \chi_0\} = 10^{-5}$, achieving a stochastic PAR of quite low 7.1 dB in a 128 carrier system. If system complexity is ignored, SLM would even reduce the stochastic discrete–time PAR by 6 dB to 6.3 dB with the same redundancy. SLM outperforms PTS in terms of PAR reduction vs. redundancy, but PTS is considerably better with respect to PAR reduction vs. additional system complexity (e.g. number of IDFTs) as it is capable to provide a greater manifold of alternative signal representations by using the same number of IDFTs together with some further vectorial additions. Obviously, complexity will be the main point of view, if practical OFDM systems are considered and so PTS (in an efficient implementational structure) will be a strong candidate.

PTS and SLM are near–optimum when PAR reduction capability vs. redundancy is considered. Thus, they seem to be the most powerful and flexible methods known to reduce OFDM peak power without nonlinear distortion.

Acknowledgement

This work was kindly supported by Ericsson Eurolab Deutschland GmbH, Nürnberg. The authors are grateful to R. Bäuml and Dr. R. Fischer for fruitful discussions.

References

[1] R. Bäuml. *Verringerung des Spitzenwertfaktors bei Mehrträgerübertragungsverfahren.* Diplomarbeit am Lehrstuhl für Nachrichtentechnik, Universität Erlangen–Nürnberg (in German), August 1996.

[2] R. Bäuml, R. Fischer, and J. Huber. Reducing the Peak–to–Average Power Ratio of Multicarrier Modulation by Selected Mapping. *Electronics Letters*, vol.32,no.22:pp.2056–2057, October 1996.

[3] M. Friese. Multicarrier modulation with low peak–to–average power ratio. *Electronics Letters*, vol.32,no.8:pp.713–714, April 1996.

[4] A. Jones, T. Wilkinson, and S. Barton. Block coding scheme for reduction of peak to mean envelope power ratio of multicarrier transmission schemes. *Electronics Letters*, vol.30,no.25:pp.2098–2099, December 1994.

[5] D. J. Mestdagh and P. M. Spruyt. A Method to Reduce the Probability of Clipping in DMT–Based Transceivers. *IEEE Trans. on Commun.*, vol.44,no.10:pp.1234–1238, October 1996.

[6] S. Müller, R. Bäuml, R. Fischer, and J. Huber. OFDM with Reduced Peak–to–Average Power Ratio by Multiple Signal Representation. *Annals of Telecommunications*, vol.52,no.1-2:pp.58–67, February 1997.

[7] S. Müller and J. Huber. *A Novel Peak Power Reduction Scheme for OFDM.* Accepted for presentation at IEEE PIMRC'97, Helsinki, Finland, September 1997.

[8] S. Müller and J. Huber. OFDM with Reduced Peak–to–Average Power Ratio by Optimum Combination of Partial Transmit Sequences. *Electronics Letters*, vol.33,no.5:pp.368–369, February 1997.

[9] P. Van Eetvelt, G. Wade, and M. Tomlinson. Peak to Average Power Reduction for OFDM Schemes by Selective Scrambling. *Electronics Letters*, vol.32,no.21:pp.1963–1964, October 1996.

[10] D. Wulich. Reduction of peak to mean ratio of multicarrier modulation using cyclic coding. *Electronics Letters*, vol.32,no.5:pp.432–433, February 1996.